

Assessment of the Contributions of Volatilization and Biodegradation to in Situ Air Sparging Performance

PAUL C. JOHNSON*

Department of Civil and Environmental Engineering, Arizona State University, Tempe, Arizona 85268-5306

In situ air sparging refers to a process in which clean air is injected directly into an aquifer formation to treat contaminant source zones, remediate dissolved contaminant plumes, or provide barriers to dissolved contaminant plume migration. This paper presents a theoretical analysis of the mechanisms and factors contributing to the overall performance of in situ air sparging systems. By examining processes occurring at the microscale, the significance of volatilization, biodegradation, bulk water flow, chemical concentrations, partitioning parameters, and air distribution are assessed. The analysis indicates that (a) if aerobic biodegradation occurs, it only enhances performance relative to the case of volatilization when dissolved contaminant concentrations are <1 mg/L, independent of other chemical parameters; (b) bulk water movement induced by water evaporation has the potential to significantly improve performance if a water velocity >2 cm/d toward the air channels occurs; (c) performance is expected to be significantly better for dissolved plumes than in sources containing immiscible phase contaminants; (d) the chemical property most affecting performance in source zones is solubility; and (e) in situ air sparging has significant potential for remediating spills of very soluble, but slowly degrading fuel oxygenates, such as MTBE.

Introduction

Over the past decade, a number of engineered soil and groundwater remediation options have been studied. The most widely used are the aeration-based technologies—soil vapor extraction and bioventing (1, 2). These utilize vapor delivery and extraction systems to promote volatilization and stimulate aerobic biodegradation of contaminants located within the vadose zone.

Equally cost-effective and proven processes for removing contaminants trapped within the capillary fringe or beneath the water table have yet to emerge. One option is to use groundwater extraction to lower the water table and then apply soil vapor extraction or bioventing to the exposed soils. Unfortunately, large groundwater extraction rates are often required for the permeable settings in which these technologies are most effective, and consequently the costs associated with above-ground water treatment and discharge can make this option impractical. Thus, a number of innovative saturated zone treatment approaches are currently under development. Of these, in situ air sparging is gaining broad appeal because it is an aeration-based technology, it appears simple to implement, and the capital costs are modest (3, 4).

In situ air sparging refers to a process in which clean air is injected directly into an aquifer as shown in Figure 1. Practitioners have proposed using in situ air sparging to (i) treat contaminant source zones, (ii) remediate dissolved contaminant plumes, or (iii) provide barriers to dissolved contaminant plume migration. In situ air sparging systems are often integrated with soil vapor extraction systems to minimize the potential for hazards caused by uncontrolled vapor migration. Proponents argue that in situ air sparging is a robust technology that offers significant cost and time savings relative to competing technologies. Others feel that its applicability may be inherently limited to idealized geologic settings where the formations are highly permeable and fairly homogeneous. There is little data from controlled studies to support either position; however, anecdotal performance reports indicate that in situ air sparging has been responsible for dissolved contaminant concentration decreases at a number of field sites (4, 5).

Most agree that there are benefits associated with the injection of air beneath the water table—it promotes volatilization, supplies oxygen for aerobic degradation, and may also induce groundwater mixing. However, there is not general agreement on the relative significance or magnitude of these processes. This paper presents a theoretical analysis of the mechanisms contributing to the overall performance of in situ air sparging systems. By examining processes occurring at the microscale, the significance of volatilization, biodegradation, mixing, chemical concentrations, partitioning parameters, and air distribution are assessed. The goal of this analysis is not to develop a predictive model for use as a design tool; rather, the goal is to examine the relative role of these processes as they contribute to remediation performance. This work is complimentary to the studies of Wilson et al. (6), who are using numerical simulation as a tool to study the governing mechanisms under specific conditions. This work is most similar to the work of Ji (7), Ahlfeld et al. (8), and Johnson (9) in that analytical solutions are developed from a simplified conceptual model. This work extends their general approach to include the effects of aerobic reactions and is not limited to linear chemical partitioning or steady-state scenarios.

Conceptual Model of Phenomena Governing Air Sparging Performance

In situ air sparging induces vapor and liquid flow, vapor- and liquid-phase diffusion, chemical partitioning, and biotic as well as abiotic chemical reactions. Each of these must be considered when developing models to assess performance. Given the current low level of understanding of these processes as they relate to in situ air sparging, it is appropriate at this point to see what can be learned from simplified conceptual models. While a simplified conceptual model may not lead to accurate prediction of the performance of any individual system, the resulting mathematical analysis may be useful for identifying those phenomena and parameters that most critically affect performance and deserve further study. It is the development of one possible simplified conceptual model and the resulting mathematical analysis that is discussed below.

Supported by flow visualization results (7, 10), it is assumed that under most field conditions (particle sizes <2 mm) the air injected into an aquifer forms a network of “channels” and “dead branches” as shown in Figure 1. The channels are active conduits for air flow from the injection point through the saturated and capillary zones and into the

* Phone: 602-965-9115; fax: 602-965-0557; e-mail: paul.c.johnson@asu.edu.

contaminant degradation reactions. Conditions d and e maximize the delivery and use of oxygen for aerobic reactions, while conditions d and f maximize the flux of the contaminant toward the air–water interface. If bulk motion of water to the air channel interface occurs after the initial water displacement by air at startup, it is most likely due to water evaporation into the flowing gas stream.

In using assumption g, it is recognized that the remediation process is a transient one in which the positions of δ and δ' are always moving; however, it is assumed that δ and δ' move slowly enough that at any time the dissolved-phase concentration profiles and fluxes may be approximated by steady-state solutions in the region bounded by $R_c < r < \delta$. The conditions under which this assumption is valid may be approximated:

$$\left(\frac{\delta^2}{D_c^{\text{eff}}}\right) < \left(\frac{C_{c,T} \rho_b \pi \delta^2}{2\pi \delta (C_{c,D} D_c^{\text{eff}}/\delta)}\right) \quad (1)$$

and

$$\left(\frac{\delta}{U_o(R_c/\delta)}\right) < \left(\frac{C_{c,T} \rho_b \pi \delta^2}{2\pi \delta U_o(R_c/\delta) C_{c,D}}\right) \quad (2)$$

where ρ_b (g of soil/cm³ of soil) denotes the soil bulk density, and D_c^{eff} (cm²/s) is the effective porous media diffusion coefficient for the contaminant in water. Equations 1 and 2 compare the characteristic times for diffusive and advective processes with the characteristic times for mass depletion by these two processes. The quantity on the left-hand side of eq 1 represents the characteristic time to establish a steady-state concentration profile by diffusion, while the quantity on the right-hand side represents the characteristic time for diffusion to deplete the contaminant within $R_c < r < \delta$. Similarly, the quantity on the left-hand side of eq 2 represents the characteristic time to establish a steady-state concentration profile by advection, while the quantity on the right-hand side represents the characteristic time for advection–dissolution to deplete the contaminant within $R_c < r < \delta$. Both eqs 1 and 2 reduce to the condition:

$$\left(\frac{2C_{c,D}}{\rho_b C_{c,T}}\right) < 1 \quad (3)$$

which simply states that the pseudo-steady-state assumption is valid as long as the amount of contaminant found in the dissolved phase is a small fraction of the total amount of contaminant present. This will hold true when dealing with strongly sorbing compounds and in situations where significant levels of immiscible-phase contaminants are present.

Assumptions a–g greatly simplify the mathematical development and allow us to reduce the governing contaminant transport equation to

$$-\left(\frac{P_i}{R}\right) \frac{dC_i^*}{dR} = \frac{1}{R} \frac{d}{dR} \left(R \frac{dC_i^*}{dR}\right) \quad (4)$$

where i can denote either dissolved oxygen ($i = O_2$) or dissolved contaminant ($i = C,D$), and

$$R = \frac{r}{R_c} \quad C_i^* = \frac{C_i}{C_i} \quad P_i = \frac{U_o R_c}{D_i^{\text{eff}}} \quad (5)$$

All parameters are as defined previously with $D_{O_2}^{\text{eff}}$ (cm²/s) denoting the effective porous media diffusion coefficient

for oxygen in water. The boundary conditions shown in Figure 2 are

$$C_{O_2}^* = 1 \quad R = 1 \quad (6a)$$

$$C_{O_2}^* = 0 \quad R = \delta'/R_c = \lambda' \quad (6b)$$

$$C_{C,D}^* = 1 \quad R = \delta/R_c = \lambda \quad (7a)$$

$$C_{C,D}^* = 0 \quad R = \delta'/R_c = \lambda' \quad (7b)$$

In the case where aerobic degradation does not occur, boundary conditions 6a and 6b are not necessary, and $\delta' = R_c$ in eq 7b.

Solutions to eq 4 can be written as

$$C_i^* = \frac{A_i}{R^{P_i}} + B_i \quad (8)$$

where A_i and B_i are integration constants to be determined by the boundary conditions. Using boundary conditions 6 and 7, eq 8 becomes

$$C_{O_2}^* = \frac{\left(\frac{\lambda'}{R}\right)^{P_{O_2}} - 1}{\lambda'^{P_{O_2}} - 1} \quad (9)$$

and

$$C_{C,D}^* = \frac{\left(\frac{\lambda \lambda'}{R}\right)^{P_c} - 1}{\lambda'^{P_c} - \lambda^{P_c}} \quad (10)$$

Assuming that any aerobic degradation reaction can be characterized by the mass β (g of contaminant/g of O₂) of contaminant required per unit mass of oxygen, then the following condition applies at the reaction interface $R = \lambda'$ ($r = \delta'$):

$$\beta^* \left[-\frac{P_{O_2}}{R} C_{O_2}^* - \left[\frac{dC_{O_2}^*}{dR} \right] \right]_{R=\lambda'} = \left[\frac{P_c}{R} C_{C,D}^* + \left[\frac{dC_{C,D}^*}{dR} \right] \right]_{R=\lambda'} \quad (11)$$

where

$$\beta^* = \left(\frac{\beta C_{O_2} D_{O_2}^{\text{eff}}}{C_{C,D} D_c^{\text{eff}}} \right) \quad (12)$$

To facilitate the mathematical solution, it is assumed at this point that $D_{O_2}^{\text{eff}} \approx D_c^{\text{eff}}$, and therefore $P_{O_2} \approx P_c = P$. This is a reasonable first-order approximation as diffusion coefficients vary roughly with the square root of molecular weight. Given this assumption, eqs 9–11 can be solved to obtain

$$\lambda'^P = \frac{(1 + \beta^*) \lambda^P}{\lambda^P + \beta^*} \quad (13)$$

which can be inserted back into eqs 9 and 10 to express both in terms of λ .

To determine how λ and λ' (or δ and δ') vary with time, a mass balance is written about the region bounded by λ and some distance ζ within the unremediated source zone. Consistent with the conceptual model, total and dissolved contaminant concentrations are uniform at $C_{c,T}$ and $C_{c,D}$, respectively. Therefore, the advective terms entering and leaving the control volume are equal, there is no diffusive

flux at $R = \zeta$ due to the uniform concentrations, and the mass balance equation becomes

$$\frac{d}{dt}[\rho_b C_{C,T}^o \pi(\zeta^2 - \delta^2)] = 2\pi\delta D_C^{\text{eff}} \left(\frac{dC_{C,D}}{dr} \right)_{r=\delta} \quad (14)$$

In writing eq 14 in this form, it is assumed that all of the contamination at the depletion zone boundary must be removed as the depletion zone grows (i.e., $C_{C,T} \rightarrow 0$). This is, of course, an approximation, as dissolved and sorbed contaminant must be left if there is to be a dissolved concentration gradient through the transport zone. However, the error introduced in making this assumption is expected to be small, based on experience with surficial soil volatilization models. For example, Thibodeaux and Hwang (11) derived volatilization equations using the pseudo-steady-state approach adopted above, while Jury et al. (12) derived equations using the more rigorous mathematical approach. In that case, the ratio of the volatilization flux predictions from the two models is $(\pi/2)^{1/2}$, suggesting that the mass balance approximation introduces little error.

Rewriting eq 14 in dimensionless form, substituting in eq 10 for $C_{C,D}$ and in eq 13 for λ' , recognizing that $\lambda = 1$ at $t = 0$, and solving yields

$$\tau = \frac{1}{P[1 + \beta^*]} \left\{ \left(\frac{\lambda^{P+2} - 1}{P+2} \right) - \left(\frac{\lambda^2 - 1}{2} \right) \right\} \quad (15)$$

where

$$\tau = \frac{t C_{C,D}^o D_C^{\text{eff}}}{\rho_b C_{C,T}^o R_C^2} \quad (16)$$

Equation 15 provides an implicit expression for $\lambda(\tau)$; thus, for any λ , the corresponding dimensionless time τ can be computed. In turn, knowledge of $\lambda(\tau)$ also provides other implicit relationships between $C_{C,D}^o$, $C_{O_2}^o$, λ' , and time through eqs 9, 10, and 13.

The only other expression needed for the discussion below is an equation for the total mass loss rate per unit channel length m (mg/cm-s) as a function of time:

$$m = 2\pi\delta \left[U_o \left(\frac{R_C}{\delta} \right) C_{C,D} + D_C^{\text{eff}} \left(\frac{dC_{C,D}}{dr} \right) \right]_{r=\delta} \quad (17)$$

Using eqs 10 and 13, eq 17 can be rewritten as

$$m^* = \frac{m}{2\pi R_C (D_C^{\text{eff}} C_{C,D}^o / R_C)} = P \left[1 + \frac{(1 + \beta^*)}{(\lambda^P - 1)} \right] \quad (18)$$

Results and Discussion

Equations 5, 12, 15, 16, and 18 are used below to assess the effects of various mechanisms and parameters on in situ air sparging performance. In this analysis, the measures of performance include mass removal rate per unit air channel length m and the radial extent of the clean zone ($\delta - R_C$) as well as changes in these quantities with time. The clean zone thickness ($\delta - R_C$) is only a valid measure of performance when diffusive transport is the dominant chemical transport mechanism. If advection-dissolution is the dominant mechanism, then most of the contaminant mass is lost from the upstream edge of the contaminant zone and the growth of δ is slow and not representative of the overall remediation.

For illustrative purposes, reasonable values are assigned to some of the parameters. For example, $C_{O_2}^o \approx 10$ mg/L, $R_C \approx 1$ cm, and $\beta \approx 0.3$ mg of contaminant/mg of O_2 are used consistently in Figures 3–6. Values for P , $C_{C,D}^o$, and $C_{C,T}^o$ are varied to examine the effects of aerobic biodegradation, advective transport, partitioning, and initial residual con-

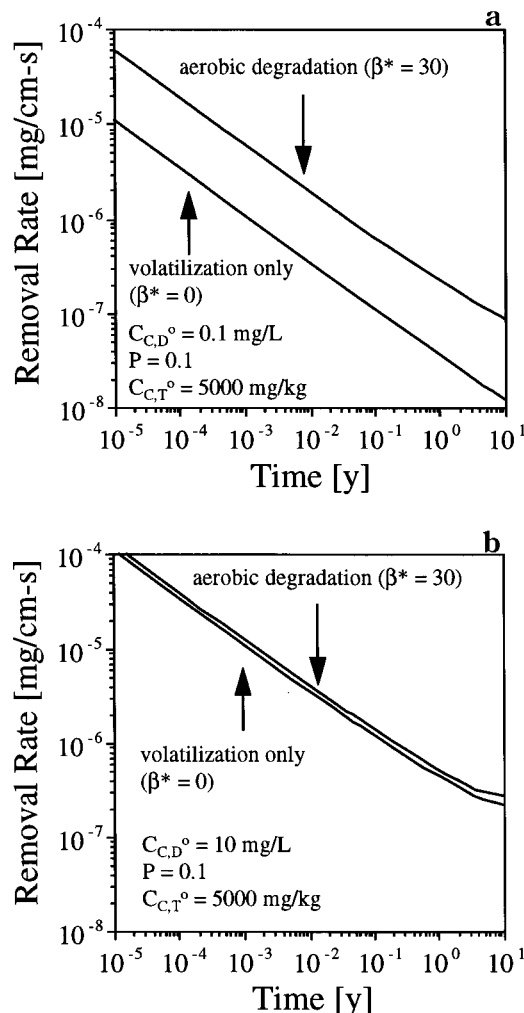


FIGURE 3. Effect of aerobic biodegradation on performance for (a) $C_{C,D}^o = 0.1$ mg/L ($\beta^* = 30$) and (b) $C_{C,D}^o = 10$ mg/L ($\beta^* = 0.3$).

centrations. Values for $C_{C,D}^o$ and $C_{C,T}^o$ were chosen to be representative of the range of conditions typical of air sparging applications to date (petroleum fuel and chlorinated solvent spill sites). Of these parameters, the value of R_C is arguably the most arbitrary; although a value of $R_C \approx 1$ cm is reasonable for coarse materials based on flow visualization experiments (7, 10). The sensitivity of the results to changes in R_C has been examined. While the specific numerical values do change with changes in R_C , the general conclusions of this analysis hold true over a reasonable range of R_C values ($0.1 < R_C < 10$ cm). While little data exist on channel sizes vs material properties, many suspect that channels are often on the order of about 10 particle diameters in width.

Relative Significance of Volatilization and Aerobic Biodegradation. The relative contributions of aerobic biodegradation and volatilization are measured by the parameter β^* . As defined by eq 12, β^* can be viewed as the maximum aerobic degradation rate resulting from oxygen diffusion into the water-saturated zone divided by the maximum volatilization rate that could result from contaminant diffusion to the air-water interface. Note that in eqs 15 and 18 β^* always appears in the term $(1 + \beta^*)$. Thus, when $\beta^* < 1$, aerobic biodegradation is insignificant and does not accelerate the remediation process relative to the case of no aerobic degradation. This effect is illustrated in Figure 3a,b, which presents the mass removal rates per unit channel length predicted by eq 18 for two different scenarios. In both cases $C_{C,T}^o = 5000$ mg/kg (a reasonable value for a source zone) and $P = 0.1$. Figure 3a compares predicted

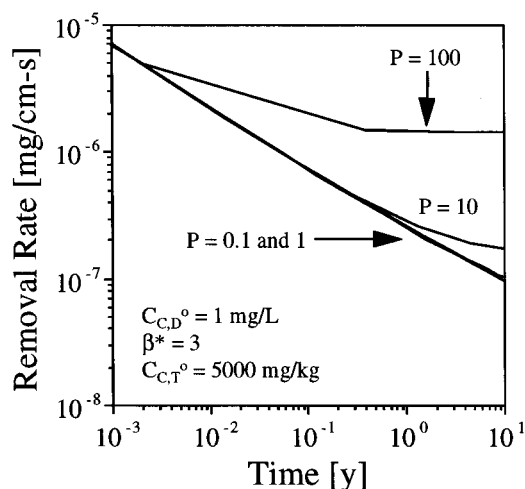


FIGURE 4. Effect of bulk water flow toward the air–water interface on performance for $C_{C,D}^0 = 1 \text{ mg/L}$ ($\beta^* = 3$), $C_{C,T}^0 = 5000 \text{ mg/kg}$, $R_c = 1 \text{ cm}$, and $D_c^{\text{eff}} = 2.5 \times 10^{-6} \text{ cm}^2/\text{s}$.

removal rates with and without aerobic biodegradation for a dissolved source concentration $C_{C,D}^0 = 0.1 \text{ mg/L}$ ($\beta^* = 30$). Figure 3b compares removal rates with and without aerobic biodegradation for a dissolved source concentration $C_{C,D}^0 = 10 \text{ mg/L}$ ($\beta^* = 0.3$). Figure 3a shows that when $\beta^* > 1$, removal is enhanced by aerobic biodegradation relative to the case of volatilization only. Figure 3b shows that when $\beta^* < 1$, the removal rate is the same with and without aerobic biodegradation. Assuming similar diffusion coefficients for oxygen and contaminant in water and assuming that $\beta \approx 0.3 \text{ mg of contaminant/mg of O}_2$ is a reasonable value for degradable compounds, then eq 12 suggests that aerobic biodegradation should be a significant mechanism at sites where $C_{C,D}^0 < 1 \text{ mg/L}$ (provided that the contaminant is readily biodegraded aerobically). Example scenarios where this condition is likely to be encountered include the dissolved plumes downgradient of gasoline spills and the source zones at heavier petroleum fuel spill sites (e.g., diesel, jet fuel, etc.).

To avoid confusion, it should be noted that volatilization cannot occur with this particular conceptual model if there is any aerobic biodegradation. If one wishes to examine the effects of having other oxygen-consuming reactions (e.g., iron precipitation), then the value of β can be modified to represent the total oxygen demand at any point in the system (β will decrease as the total noncontaminant oxygen demand increases).

Effect of Bulk Water Movement on Performance. The effect of bulk water movement toward an air channel on performance is measured by the Peclet number P appearing in eqs 15 and 18. As defined by eq 5, P represents the ratio of advective and diffusive transport. To examine how changes in this parameter affect performance, consider Figure 4. Here, removal rates per unit air channel length are presented for $0.1 < P < 100$, $C_{C,D}^0 = 1.0 \text{ mg/L}$ ($\beta^* = 3$), and $C_{C,T}^0 = 5000 \text{ mg/kg}$. As can be seen, advection enhances performance relative to the diffusion-only case only when $P > 10$. If aerobic biodegradation was not occurring ($\beta^* = 0$), enhancement in performance is observed for $P > 1$. For reference, given $R_c = 1 \text{ cm}$ and $D_c^{\text{eff}} \approx 2.5 \times 10^{-6} \text{ cm}^2/\text{s}$, $P=10$ corresponds to a velocity at the air–water interface $U_o \approx 2 \text{ cm/d}$. As stated previously, if there were to be bulk flow toward the air–water interface, it would most likely be a result of water evaporation into the flowing air stream. Given that typical air sparging air injection rates fall in the range of 30–600 L/min per well and that most air is injected at less than 100% relative humidity, there is great potential for bulk flow due to water evaporation to be a significant contributor to remediation by in situ air sparging.

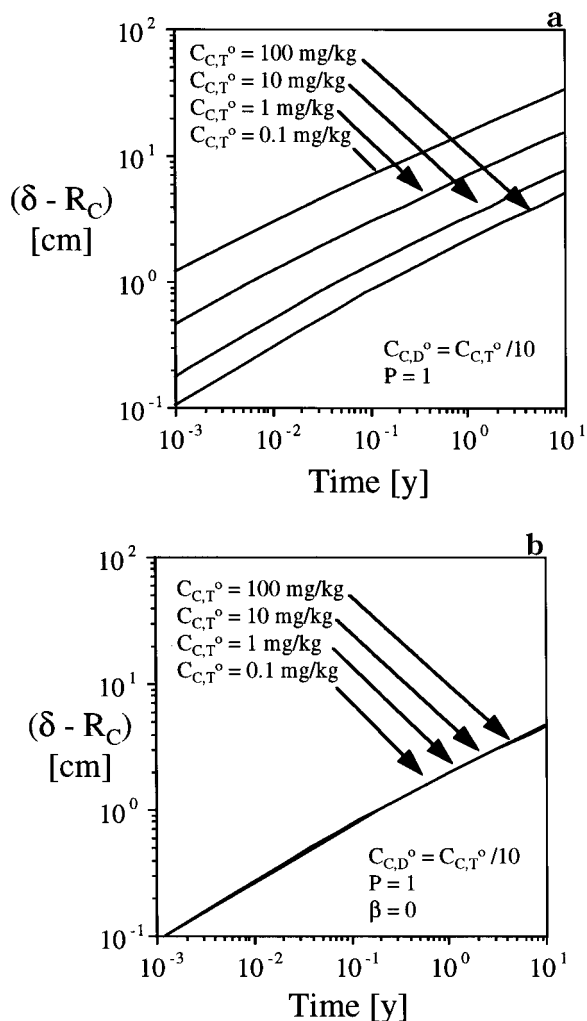


FIGURE 5. Effect of initial residual concentration $C_{C,T}^0$ on performance for $C_{C,D}^0 = C_{C,T}^0/10$, $R_c = 1 \text{ cm}$, $P = 1$: (a) aerobic biodegradation and (b) no biodegradation.

Effect of Initial Residual Contaminant Concentration on Performance. Figure 5a,b is presented to help illustrate how performance is affected by the starting residual contaminant concentration $C_{C,T}^0$, for situations in which the dissolved and total contaminant concentrations are linearly related. Here performance is being measured by the increase in $(\delta - R_c)$ with time, as opposed to mass removal rate used in Figures 3 and 4. Increases in $(\delta - R_c)$ reflect a growth in the zone of remediated soil surrounding the air channel. Also, the results displayed in Figure 5a,b correspond to the case of linear partitioning where $C_{C,D}^0 = C_{C,T}^0/10$ and $P = 1$. For reference, linear partitioning would be expected to occur in a dissolved plume rather than a source zone. The only difference between Figure 5, panels a and b, is that the results in Figure 5a include aerobic biodegradation, while the results in Figure 5b correspond only to mass loss through volatilization. Figure 5a would be most representative of conditions at petroleum fuel sites, while Figure 5b would be most representative of conditions at chlorinated solvent spill sites.

Figure 5a,b suggests that, under linear partitioning conditions, the initial residual concentration significantly affects performance only when the contaminant is aerobically degradable. As in the case of Figure 3a, the relative contribution of biodegradation to remediation becomes more important as the dissolved contaminant concentration decreases. In Figure 5a, the four initial residual contaminant concentrations in increasing order correspond to $\beta^* = 300$, 30, 3, and 0.3. Thus, enhancements in performance with

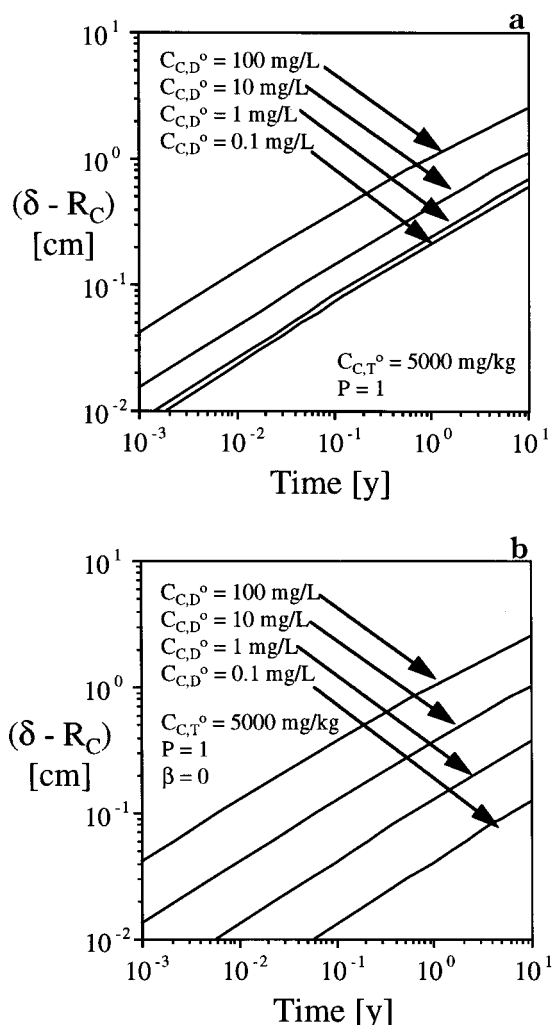


FIGURE 6. Effect of solubility on performance for $C_{C,T} = 5000$ mg/kg, $R_c = 1$ cm, $P = 1$: (a) aerobic biodegradation and (b) no biodegradation.

decreasing $C_{C,T}$ would be expected for the three lowest residual contaminant concentrations.

Effect of Solubility and Sorption on Performance. Figure 6a,b illustrates how remediation performance is expected to be affected by solubility for a fixed $C_{C,T} = 5000$ mg/kg. As in Figure 5a,b, performance is being measured by the increase in $(\delta - R_c)$ with time. For reference, partitioning of this type would be expected to occur in source zones containing immiscible-phase contaminants. Once again, the only difference between Figure 6, panels a and b, is that the results in panel a include aerobic biodegradation, while the results in panel b correspond only to mass loss through volatilization.

Both Figure 6, panels a and b, show an increase in performance with increasing solubility. In the case of Figure

6a, however, performance reaches a lower asymptote as $C_{C,D} < 1$ mg/L. This again is a reflection of the importance of aerobic biodegradation when $C_{C,D} < 1$ mg/L. These results imply that the remediation performance would be expected to be similar for compounds having different solubilities, provided that the compounds were aerobically degradable, that $C_{C,D} < 1$ mg/L, and that the initial residual concentrations were similar. Conversely, performance would be expected to always decrease as solubility decreases for non-degradable compounds.

Figure 6a,b can also be viewed as indicating the effect of changing soil sorption coefficient K_s , where $K_s = (C_{C,T}/C_{C,D})$. In that case, these figures indicate that performance always decreases with increasing sorption coefficient, except in the case where compounds are aerobically degradable.

It is useful to note at this point that one key feature of this approach is that predicted removal rates do not depend on standard physical/chemical measures of volatilization, such as vapor pressure and Henry's law constants. In fact, this model indicates that chemicals having relatively low Henry's law constants but high solubilities (e.g., fuel oxygenates like MTBE) may be good targets for remediation by in situ air sparging.

Literature Cited

- (1) Johnson, P. C.; Stanley, C. C.; Kemblowski, M. W.; Byers, D. L.; Colthart, J. D. *Ground Water Monit. Rev.* **1990**, 10 (2), 159–178.
- (2) Hincsee, R. E.; Ong, S. K. *J. Air Waste Manage. Assoc.* **1992**, 42 (10), 1305–1312.
- (3) Johnson, R. L.; Johnson, P. C.; McWhorter, D. B.; Hincsee, R. E.; Goodman, I. *Ground Water Monit. Rem.* **1993**, 13 (4), 127–135.
- (4) Marley, M. C.; Bruell, C. J. *In Situ Air Sparging: Evaluation of Petroleum Industry Sites and Considerations for Applicability, Design, and Operation*; API Publication 4609; American Petroleum Institute: Washington, DC, 1995.
- (5) Bass, D. H.; Brown, R. A. Presented at the National Ground Water Association Petroleum Hydrocarbons and Organic Chemicals in Ground Water Conference, Houston, TX, November 1995.
- (6) Wilson, D. J.; Gomez-Lahoz, C.; Rodriguez-Maroto, J. M. *Sep. Sci. Technol.* **1994**, 29, 2387.
- (7) Ji, W. Ph.D. Dissertation. University of Connecticut at Storrs, 1994.
- (8) Ahlfeld, D. P.; Dahmani, A.; Ji, W. *Ground Water Monit. Rem.* **1994**, 14 (4), 132–139.
- (9) Johnson, R. L. In *Air Sparging for Site Remediation*; Hincsee, R. E., Ed.; Lewis Publishers: Boca Raton, FL, 1994; pp 14–22.
- (10) Ji, W.; Dahmani, A.; Ahlfeld, D.; Lin, J. D.; Hill, E. *Ground Water Monit. Rem.* **1993**, 13 (4), 115–126.
- (11) Thibodeaux, L. J.; Hwang, S. T. *Environ. Prog.* **1982**, 1, 42–46.
- (12) Jury, W. A.; Russo, D.; Streile, G.; El Abd, H. *Water Resour. Res.* **1990**, 26, 13–20.

Received for review June 2, 1997. Revised manuscript received September 22, 1997. Accepted September 25, 1997.*

ES9704850

* Abstract published in *Advance ACS Abstracts*, November 1, 1997.